Article

Polyaniline/FeO Nanoparticle Composite: Synthesis and Reaction Mechanism

Chunhui Yang, Jingjie Du, Qian Peng, Ruirui Qiao, Wei Chen, Chuanlai Xu, Zhigang Shuai, and Mingyuan Gao

More About This Article

Additional resources and features associated with this article are available within the HTML version:

- Supporting Information
- Access to high resolution figures
- Links to articles and content related to this article
- Copyright permission to reproduce figures and/or text from this article

View the Full Text HTML

Polyaniline/Fe$_3$O$_4$ Nanoparticle Composite: Synthesis and Reaction Mechanism

Chunhui Yang,[†] Jingjie Du,[‡] Qian Peng,[†] Ruirui Qiao,[†] Wei Chen,[‡] Chuanlai Xu,*,[‡]
Zhigang Shuai,[†] and Mingyuan Gao*,[†]

Institute of Chemistry, Chinese Academy of Sciences (CAS), Zhong Guan Cun, Bei Yi Jie 2, Beijing 100190, China, and School of Food Science and Technology, Jiangnan University, Wuxi, Jiangsu 214122, China

Received: December 17, 2008; Revised Manuscript Received: February 4, 2009

Polyaniline/Fe$_3$O$_4$ nanoparticle composite was prepared by polymerizing aniline in the presence of Fe$_3$O$_4$ nanoparticles upon the use of H$_2$O$_2$ as oxidant. The polymerization was monitored by ultraviolet−visible absorption spectroscopy. The microstructure of the resultant composite was characterized by transmission electron microscopy. The molecular structure of the resultant polyaniline in the composite was investigated by both Fourier transform infrared spectroscopy and X-ray photoelectron spectroscopy, while the magnetic property of the composite was characterized by vibrating sample magnetometer. Furthermore, the microwave absorption property of the resultant composite was measured in a frequency range of 2−18 GHz. Systematic investigations revealed that carboxylic acid in the buffer presented a determined role in the polymerization of aniline. To discover the role of carboxylic acid in the polymerization of aniline, more control experiments were designed and carried out by theoretical calculation in combination with electron spin resonance measurements. It was for the first time found out that carboxylic acid such as acetic acid and succinic acid can not only catalyze the polymerization of aniline but also facilitate the generation of hydroxyl radical via the decomposition of H$_2$O$_2$.

Introduction

Organic−inorganic hybrid materials exhibiting both electric and magnetic properties are very useful for electromagnetic shielding and microwave absorption.[1−4] Because magnetic iron oxide nanoparticles present many special properties superior to molecular magnetic materials, to dope conducting polymer with magnetic iron oxide nanoparticles remains a hot area. In general, two synthetic routes have been established to achieve composite materials composed of conducting polymers and magnetic iron oxide particles. The first type of method relies on the in situ formation of magnetic iron oxide particles in the presence of conducting polymer upon chemical reactions, such as hydrolysis of Fe(II) and Fe(III) ions, while the second type of method is based on the polymerization of monomers in the presence of magnetic iron oxide nanoparticles. In comparison with the first type of synthetic routes, the second one offers better control over the magnetic properties of the resultant hybrid materials.

Polyaniline (PANI) as a conducting polymer has become very attractive because of its facile synthesis,[5] stable chemical and environmental properties,[6] and inherent reversible doping/dedoping states.[7] Therefore, it is a suitable matrix for achieving electromagnetic shielding or absorption materials by doping with magnetic iron oxide nanoparticles. PANI is commonly synthesized by oxidizing aniline monomer in acid solution via either chemical or electrochemical method.[5] In comparison with electrochemical method, the chemical synthesis of PANI is widely used for mass production.[5] Various types of oxidants such as (NH$_4$)$_2$S$_2$O$_8$,[6,8,9] FeCl$_3$,[10,11] K$_2$Cr$_2$O$_7$,[9,12] KIO$_3$,[9] and H$_2$O$_2$,[9] can be used in the chemical synthesis of PANI. Among these

oxidants, (NH$_4$)$_2$S$_2$O$_8$ is the most commonly used one, but the resultant PANI is often neither soluble nor fusible. In addition, the posttreatments of the products for eliminating inorganic byproduct, such as ammonium sulfate, are rather complicated. Therefore, from the point of view of environmental friendliness, H$_2$O$_2$ is an ideal oxidant since its reduction product is only water. However, when H$_2$O$_2$ is used alone, the reaction rate for forming PANI is extremely slow. Therefore, it is generally believed that it is impossible to prepare PANI through the oxidation of aniline by using H$_2$O$_2$ alone at room temperature.[13]

To improve the reactivity of H$_2$O$_2$, two different kinds of catalysts are often used in the preparation of PANI, i.e., Fenton and Fenton-like reagents (Fe^{2+}/Fe^{3+})[13,14] or horseradish peroxidase (HRP).[15−18] It has been demonstrated that the Fenton reagent takes effect by accelerating the decomposition of hydroxyl peroxide to generate hydroxyl radicals.[13,14] In contrast, Fe^{3+} in the active center of HRP catalyzes the oxidation of aromatic amines and phenols via the binding of H$_2$O$_2$ to generate free radicals of substrate molecules. Then, the resultant substrate radicals undergo coupling reaction to produce the dimer. Thereafter, upon further oxidation and coupling reactions with monomer, dimer, and even oligomer, polymer is eventually formed.[19] So far, there have been a large number of papers about HRP-based syntheses of polyphenol and PANI.[15] Although enzymes are generally characterized by excellent substrate specificity in comparison with conventional catalysts, the use of HRP remains more costly than Fenton reagent.

Very recently, Gao et al. reported that Fe$_3$O$_4$ nanoparticles exhibit an intrinsic peroxidase-like activity,[20] which inspired us to use Fe$_3$O$_4$ nanoparticles as catalyst to prepare composite material composed of PANI and Fe$_3$O$_4$ nanoparticles. The microwave absorption property of the resultant composite material was demonstrated. Furthermore, systematic experiments in combination with theoretical calculations were carried out

* To whom correspondence should be addressed. Prof. Mingyuan Gao and Prof. Chuanlai Xu. Phone: 86-10-62625212 (M.G.). Fax: 86-10-82613214 (M.G.); 86-510-85329076 (C.X.). E-mail: gaomy@iccas.ac.cn (M.G.); xcl@jiangnan.edu.cn (C.X.).
  [†] CAS.
  [‡] Jiangnan University.

Polyaniline/Fe$_3$O$_4$ Nanoparticle Composite

J. Phys. Chem. B, Vol. 113, No. 15, 2009 **5053**

to elucidate the nature of "peroxidase-like activity" of Fe$_3$O$_4$ nanoparticles.

Experimental Section

Materials. Aniline of analytical grade was supplied by Sinopharm Chemical Co., Ltd., Shanghai, China. Poly(sodium 4-styrenesulfonate) (SPS, M$_w$ = 70000) was purchased from ACROS. Other reagents used were commercially available products with the highest purities. Fe$_3$O$_4$ nanoparticles were prepared as described in a previous publication.[21] The average diameter of the particles determined by transmission electron microscope was 11.1 ± 1.4 nm. Because the resultant Fe$_3$O$_4$ nanoparticles were chemically modified by poly(ethylene glycol) (PEG, M$_n$ = 2000), they presented excellent solubility and colloidal stability in aqueous solution.[21] Throughout the following preparations, practically no particle aggregation was observed. 5-(Diethoxyphosphoryl)-5-methyl-1-pyrroline-*N*-oxide (DEPMPO), used as a spin trap in the electron spin resonance measurements, was synthesized according to a literature procedure.[22]

Synthesis of PANI/Fe$_3$O$_4$ Nanoparticle Composite. The polymerization of aniline was carried out at room temperature as follows. Typically, 3 mL of buffer solution (pH 2.5) containing 0.018 mmol of aniline, 0.018 mmol of SPS, and 0.45 mg of Fe$_3$O$_4$ nanoparticles was prepared. Then, 900 μL of 80 mM H$_2$O$_2$ was intermittently injected (50 μL/5 min). The polymerization was normally allowed for 20 h after the introduction of H$_2$O$_2$. After that, the reaction was terminated with a 4-fold volume of isopropyl alcohol to precipitate the composite, which was subsequently collected via centrifugation at 2000 rpm. After being thoroughly washed with ethyl ether for three times, the composite material was dried for further characterizations. For microwave absorption, saturation magnetization, and X-ray photoelectron spectroscopy measurements, the samples were prepared simply by scaling up the above-mentioned reaction system by 120 times.

Microwave Absorption Measurements. A powder sample of composite material was first mixed with an equal weight of olefin. Then, the resultant mixture was used to form an O-ring-shaped sample (i.d. = 3 mm, o.d. = 7 mm, and thickness = 2 mm) under the melting state of olefin. The relative complex permittivity and the relative complex permeability were determined using an HP8722ES vector network analyzer in the range of 2−18 GHz.

Computational Method. To elucidate the reaction mechanism, the equilibrium geometries of all the compounds were optimized at the level of closed shell by Kohn−Sham density functional theory (DFT). The B3LYP functional and the basis set 6-31++G* were used. All calculations were carried out by use of the Gaussian 03 program package (Revision B.03).

Characterizations. Ultraviolet−visible (UV−vis) absorption spectra were recorded with a Cary 50 spectrometer. Transmission electron microscopy (TEM) images were recorded with a JEM-100CX II microscope operating at an accelerating voltage of 100 kV. Fourier transform infrared (FTIR) spectra were recorded on a Bruker EQUINOX55 FT-IR spectrometer using KBr pellet. X-ray photoelectron spectroscopy (XPS) measurements were performed on a VG ESCALAB 220i-XL spectrometer. All binding energies for different elements were calibrated with respect to the C1s line at 284.8 eV from the contaminant carbon. A Shirley-type background was used during curve fitting. All fittings were carried out using Voigt-shaped peaks with an equal full width at half-maximum (fwhm) for each data set. The magnetic hysteresis loops of the resultant capsules were recorded with a vibrating sample magnetometer (VSM, JDM-
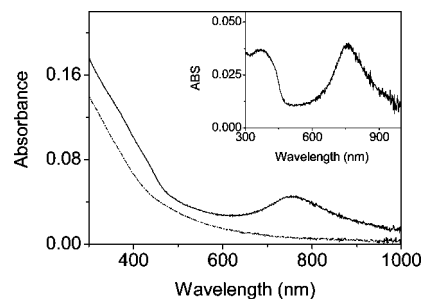

Figure 1. UV−vis absorption spectra of the reaction mixture recorded before (dashed line) and after (solid line) the polymerization of aniline which had taken place for 21 h in citric acid/disodium hydrogen phosphate buffer (pH 2.5) in the presence of Fe$_3$O$_4$ nanoparticles. Inset: the difference between the solid line and dashed line spectra.

13). The iron contents in the Fe$_3$O$_4$ particles and the resultant composite were determined by thermogravimetric analysis (TGA, Perkin-Elmer TGA) and inductive coupled plasma (ICP) emission spectrometer (IRIS Intrepid II XSP, Thermo Electron Co.), respectively. The electron spin resonance (ESR) signals were recorded on an ESP300 (Bruker Co.) at room temperature.

Results

Polymerization of Aniline in the Presence of Fe$_3$O$_4$ Nanoparticles. The first set of experiments was performed basically according to those reported by Gao et al.[20] except that the Fe$_3$O$_4$ nanoparticles were prepared by a different synthetic route. In addition, citric acid/disodium hydrogen phosphate buffer was chosen instead of acetic acid/sodium acetate due to its wide pH buffering window of 2.5−9.0, because the pH value of the reaction system not only influences the doping state of PANI, but also alters the redox reactivity of H$_2$O$_2$. The whole polymerization reaction was monitored by UV−vis spectrometer. Figure 1 shows a typical absorption spectrum of the reaction system recorded at pH 2.5 21 h after H$_2$O$_2$ was completely introduced. By subtracting that recorded before polymerization, two absorption bands peaking at 370 and 760 nm appear as shown in the inset of Figure 1. The first one can be attributed partly to the π−π* transition of the benzenoid ring and partly to polaron band transistion due to its broad feature, while the second one can be assigned to polaron band transition, suggesting that conducting PANI was formed.[16,18,23]

Optimization of pH. Five additional parallel experiments were carried out upon the use of 0.1 M citric acid and 0.2 M disodium hydrogen phosphate buffer at pH 3.5, 4, 7, 8, and 9, respectively, to show the pH-dependent polymerization behavior of aniline, while the other synthetic parameters remained unchanged. Detailed results reveal that the polymerization only occurred around pH 2.5, and no evident polymerization was practically observed at pH ≥ 3.5 with respect to the current citric acid/disodium hydrogen phosphate buffer system (data not shown). Therefore, the following syntheses were carried out at pH 2.5.

Optimization of the Molar Ratios among Different Reagents. SPS is a widely used PANI template.[24] According to previous study, when the molar ratio of aniline to SPS is lower than 1:1 (the aniline to SPS ratio mentioned here and below is referring to the molar ratio between aniline monomer and the repeat unit of SPS), there will not be enough aniline monomers aligning along the SPS template, consequently leading to oligomer.[16] However, no significant effects were observed when the molar ratio of aniline to SPS was higher than 1:1 (data not shown). Therefore, the molar ratio was fixed to 1:1 for the following experiments.
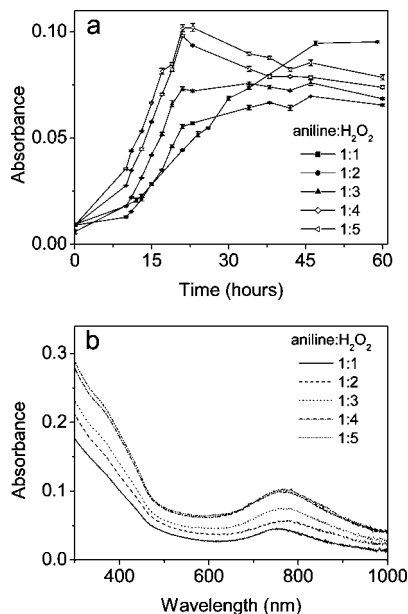
Figure 2. (a) Temporal evolutions of the absorbance around 760 nm recorded from different reaction mixtures; (b) UV−vis absorption spectra of reaction mixtures recorded after the polymerization of aniline had taken place for 20 h.

Figure 3. TEM images of the preformed Fe_3O_4 nanoparticles (a) and those remaining in the resultant composite (b).

Figure 4. FTIR spectrum of the as-prepared PANI/Fe_3O_4 nanoparticle composite.

Figure 5. XPS N1s core-level spectrum of the PANI/Fe_3O_4 nanoparticle composite together with the best fits in different line styles.

According to the reference report,[16] the concentration of aniline was set to 6 mM. Then, the molar ratio between aniline and H_2O_2 was optimized in a range of 1:1−1:5. The results shown in Figure 2a suggest that when the ratio is lower than 1:3, the reaction systems present enhanced efficiency and maximal conversions at around 20 h, derived from the absorbance variation at 760 nm. Furthermore, the ratios of 1:4 and 1:5 do not give rise to a big difference as more clearly shown in Figure 2b; therefore, the molar ratio between aniline and H_2O_2 was set as 1:4 for the following experiments, which means the molar ratio of aniline:SPS:H_2O_2 was 1:1:4.

Yield of the Reaction under Optimized Conditions. The yield of the polymerization occurring under optimized conditions was estimated by comparing the mass of all reactants including aniline, SPS, and Fe_3O_4 nanoparticles with that of the composite material eventually obtained, while the amount of SPS was considered to be completely transferred into the PANI-based composite. The final results suggested that the reaction yield under optimized conditions was quite close to 80%.

Microstructure of the PANI/Fe_3O_4 Composite Material. The general morphology of the preformed Fe_3O_4 nanoparticles and the resultant PANI/Fe_3O_4 nanoparticle composite was characterized by TEM. As shown in Figure 3, the preformed Fe_3O_4 nanoparticles are rather uniform in size with an average particle size of 11.1 ± 1.4 nm, while in the composite Fe_3O_4 nanoparticles that survived present a slightly decreased particle size of 10.1 ± 1.2 nm due to the corrosion at pH 2.5, which suggests that it should be possible to further alter the physical properties of the resultant composite by varying the size and content of the Fe_3O_4 nanoparticles.

Structural Characteristics of PANI in the Resultant Composite. Figure 4 shows the FTIR spectrum of the PANI/Fe_3O_4 composite obtained under optimized conditions. The absorption bands peaking at 1602 and 1500 cm^{-1} can be assigned to the quinonoid ring and the benzenoid ring, respectively.[16,23] Because the relative absorbance intensity of the quinonoid ring is greater than that of the benzenoid ring, it can be deduced that PANI in both pernigraniline form and
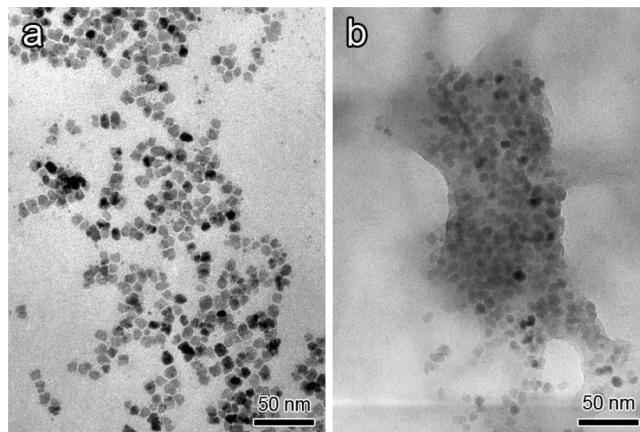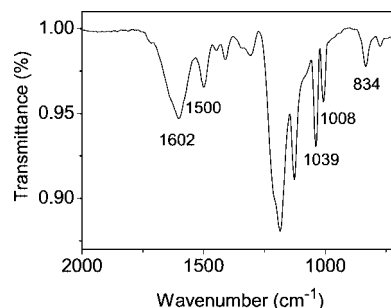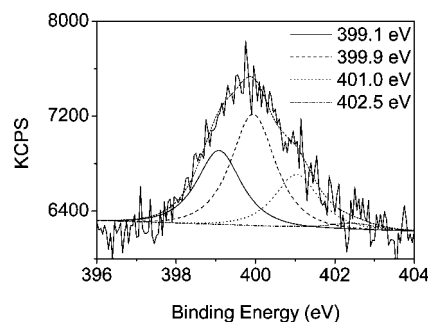
emeraldine form are coexisting in the resultant composite. The appearance of the C−H out-of-plane bending vibrational band of the 1,4-ring at 834 cm^{-1} suggests that a head-to-tail configuration is taken by PANI prepared in the current reaction system,[16,23] which is further supported by the absence of vibrational bands for 1, 2 and 1, 2, 4 substitutions of the benzenoid ring at around 740 and 910 cm^{-1}, respectively. The appearances of the asymmetric and symmetric stretching vibrational bands of S=O at 1039 and 1008 cm^{-1} demonstrates that SPS is presented the resultant composite.[16] These assignments, very well in agreement with previous investigations, imply that both pernigraniline and emeraldine were formed.[25,26]

The intrinsic redox states of resultant PANI were further analyzed by fitting the N1s signal of the XPS spectrum. Detailed results are given in Figure 5, and the N1s signal is fitted by four peaks at 399.1 eV (30.34%), 399.9 eV (45.72%), 401.0 eV (21.54%), and 402.5 eV (2.40%), respectively. According to literature results, the first two peaks at 399.1 and 399.9 eV can be assigned to undoped quinonoid imine (-N=) and benzenoid amine (-NH-), respectively,[27] while the other two
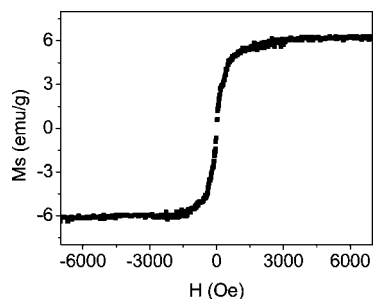
Figure 6. Hysteresis loop of the as-prepared PANI/Fe₃O₄ nanoparticle composite recorded at room temperature.
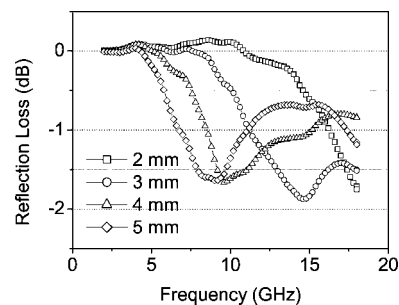

Figure 7. Simulation of reflection loss spectra of the PANI/Fe₃O₄ nanoparticle composite dispersed in olefin of different thickness by 50 wt %.

signals, 401.0 and 402.5 eV, can be attributed to iminium and radical cation amine groups.[23] The fitting results not only provide consistent support for the coexistence of pernigraniline and emeraldine as concluded on the basis of the FTIR results but also allow further evaluation of the doping level of PANI in the PANI/Fe₃O₄ composite.[23,28] According to the ratio of N^+/N, it can be concluded that 23.9% of PANI was protonated.

Magnetic Properties of Fe₃O₄ Nanoparticles Embedded in PANI. A magnetic hysteresis loop of the composite material, as shown in Figure 6, was recorded at room temperature. In comparison with the preformed Fe₃O₄ nanoparticles, the saturation magnetization (M_s) of the PANI/Fe₃O₄ composite drops from 40.4 to 6.2 emu/g. Taking the Fe₃O₄ contents in both preformed particle sample (47.2%) and PANI/Fe₃O₄ composite (8.8%) into consideration, nearly 80% of the initial saturation magnetization was preserved after Fe₃O₄ nanoparticles were embedded in PANI.

Microwave Absorption of PANI/Fe₃O₄ Composite. The real part of permittivity ε' and the imaginary part ε'' of the relative complex permittivity ε ($\varepsilon = \varepsilon' - j\varepsilon''$), as well as the real part of permeability μ' and the imaginary part μ'' of the relative complex permeability μ ($\mu = \mu' - j\mu''$) of PANI/Fe₃O₄ composite were measured with the aid of a vector network analyzer within a frequency range of 2−18 GHz. Detailed results are provided in Figure S1 in the Supporting Information. The electromagnetic reflection loss of the composite material was simulated according to transmission line theory. The electromagnetic reflection loss R is defined as

$$R = 20 \log \left| \frac{Z_{in} - Z_0}{Z_{in} + Z_0} \right| \quad (1)$$

where Z_{in} is the normalized input impedance at the interface of the free space and the composite material and Z_0 is the characteristic impedance of free space. Z_{in} and Z_0 are expressed by eqs 2 and 3, respectively.

$$Z_{in} = \sqrt{\frac{\mu_0 \mu}{\varepsilon_0 \varepsilon}} \tanh(j2\pi f t \sqrt{\mu_0 \mu \varepsilon_0 \varepsilon}) \quad (2)$$

$$Z_0 = \sqrt{\frac{\mu_0}{\varepsilon_0}} \quad (3)$$

where μ is relative complex permeability, ε is relative complex permittivity, f is the frequency of microwave, t is the thickness of the composite material, and μ_0 ($4\pi \times 10^{-7}$ N/A²) and ε_0 (8.85×10^{-12} F/m) are constants. According to eq 1, the electromag-

netic reflection losses of the composite material with different thickness are shown in Figure 7. In general, the electromagnetic reflection loss R presents a thickness-dependent behavior and moves to a low-frequency direction against the sample thickness. The maximum reflection loss R reaches −2 dB at 14.6 GHz when $t = 3$ mm. Although R remains lower than that reported in literature,[29] it remains improvable that the content of Fe₃O₄ nanoparticles in the composite material is only of 8.8%.

Discussion

In fact, the greatest motivation for us as well as other groups to follow the investigations of Gao et al. was because they observed that Fe₃O₄ nanoparticles possessed an intrinsic peroxidase-like activity. If this is true, the magnetic iron oxide nanoparticles will be greatly desirable for developing new materials due to their magnetic properties and "biological functions". Therefore, it is necessary to carefully investigate the mechanism of the reaction "catalyzed" by Fe₃O₄ particles.

Catalytic Behavior of Carboxylic Acids. It was previously reported that the properties of PANI are strongly associated with the nature of the acid used for preparation.[30−32] Therefore, under optimized pH 2.5, additional buffering systems were also adopted apart from citric acid/disodium hydrogen phosphate. They were 0.45 M acetic acid/sodium acetate, 0.225 M succinic acid/sodium succinate, 0.15 M citric acid/sodium citrate, and 0.1 M phosphate acid/sodium dihydrogen phosphate. The buffering systems except for the last one were prepared in a way in which the concentrations of carboxylic group were set to be identical.

The results shown in Figure 8 demonstrate that in the presence of Fe₃O₄ nanoparticles the polymerizations of aniline occurred except for the phosphate buffer in which only oligomeric PANI was formed. Even though the acetate buffer and the succinate buffer present higher efficiency than the citrate buffer, it is still reasonable to conclude that carboxylic acid plays a very important role in the polymerization reaction of aniline since PANI was hardly formed in the phosphate buffer.

The control experiments performed in the absence of Fe₃O₄ nanoparticles however suggest that the polymerization of aniline can effectively occur in the former two buffering systems with a comparable (succinate buffer) or a little lower efficiency (acetate buffer). Therefore, it can be concluded that the carboxylic acid also plays a catalyzing role in the polymerization reaction of aniline. With respect to the citrate buffer, that nearly no PANI was formed could probably be attributed to the steric effect of triacid (citric acid) in comparison with monoacid (acetic acid) and diacid (succinic acid).

Mechanism for the Catalytic Behavior of the Carboxylic Acids. Based on the aforementioned results as well as those reported in literatures,[20,33] the experimental observations can be
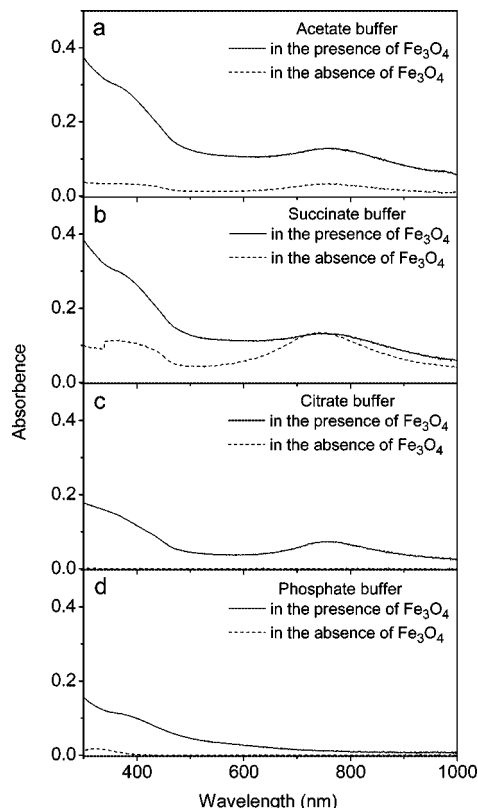
Figure 8. Absorption spectra of reaction mixtures formed by different types of buffers. The reactions were allowed to take place at pH 2.5 for 20 h after the introduction of H_2O_2.

Figure 9. HOMO orbitals of aniline (phNH$_2$), aniline radical cation (phNH$_2^{\bullet+}$), phNH$_2$/CH$_3$COO$^-$, and phNH$_2^{\bullet+}$/CH$_3$COO$^-$, together with their HOMO levels.

summarized as follows. The "peroxidase-like" behaviors of Fe_3O_4 particles were mainly observed in buffers containing various types of organic acid such as acetic acid[20,33] and citric acid.[20] However, the Fe_3O_4 nanoparticles lost their peroxidase-like activity in the phosphate buffer, as shown in Figure 8d. Moreover, the polymerization of aniline which is also a typical HRP-catalyzable reaction can effectively take place in the presence of organic acid such as acetic acid and succinic acid with no Fe_3O_4 particles being presented. All these experimental observations imply that the role of carboxylic acid is one of the most important issues for discovering the mechanism of peroxidase-like activity of Fe_3O_4 nanoparticles.

In principle, the chemical nature of the chromometry used in HRP-based reaction is to form a dimer or oligomer of substrates such as 3,3,5,5-tetramethylbenzidine (TMB), *o*-phenylenediamine (OPD), and 3,3′-diaminobenzidine (DAB), which as typical chromogens for HRP are just derivatives of aniline. Therefore, the catalytic mechanism of carboxylic acids with respect to aniline will identically be applicable to HRP chromogens. With respect to the polymerization of aniline, it is commonly accepted that the oxidation of aniline monomer to form dimeric species is the rate-limiting step.[34] Therefore, the interactions between the following species, i.e., aniline/acetic acid (phNH$_2$/CH$_3$COOH), aniline radical cation/acetic acid (phNH$_2^{\bullet+}$/CH$_3$COOH), aniline/acetic anion (phNH$_2$/CH$_3$COO$^-$), and aniline radical cation/acetic anion (phNH$_2^{\bullet+}$/CH$_3$COO$^-$) were calculated by frontier molecular orbital theory. Detailed results reveal that CH$_3$COO$^-$ can form stable complexes with phNH$_2$ and phNH$_2^{\bullet+}$, respectively, resulting in the increases of the HOMO energy from -6.87 to -1.88 eV for phNH$_2$ and from -7.02 to -3.45 eV for phNH$_2^{\bullet+}$. The optimized structures of phNH$_2$/CH$_3$COO$^-$ and phNH$_2^{\bullet+}$/CH$_3$COO$^-$ complexes are shown in Figure 9. The great increases of the HOMO energies
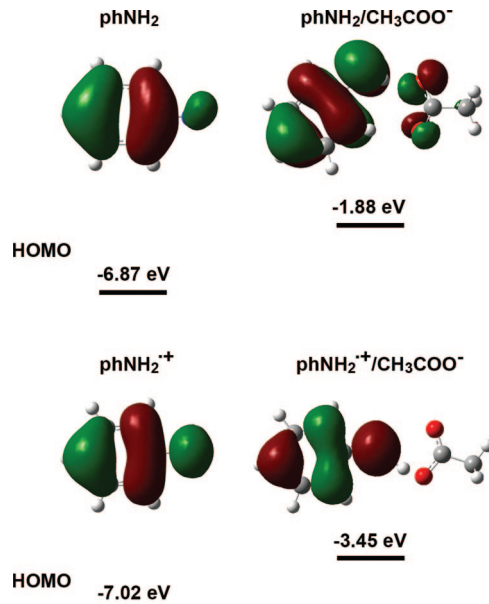
will substantially enhance the reactivity of both phNH$_2$ and phNH$_2^{\bullet+}$ in the oxidation and the dimeric reactions, respectively, which well-interprets the catalytic behavior of the carboxylic acids.

Although the presence of Fe_3O_4 nanoparticles did not enhance the polymerization efficiency of aniline in the succinate buffer, the particles contribute to the polymerization efficiency in the acetate buffer that was used to demonstrate the peroxidase-like activity of Fe_3O_4 particles, which suggest that Fe_3O_4 nanoparticles also have an effect in catalyzing the polymerization of aniline in the acetate buffer.

It should be pointed out that, under the optimized pH 2.5, Fe_3O_4 nanoparticles will be partly dissolved due to the acidic corrosion. Fe^{2+} and Fe^{3+} are consequently available for catalyzing the reaction of aniline following the principle of Fenton or Fenton-like reagent by accelerating the decomposition of H_2O_2 to generate hydroxyl radical.[14,35] To further elucidate this contribution, ESR measurements were performed to detect radicals formed in the following systems upon the use of DEPMPO as a spin trap, i.e., the acetate buffer solution containing no Fe_3O_4 nanoparticle, leaching solutions from phosphate buffer, and acetate buffer containing Fe_3O_4 nanoparticles. In all these mimic systems, equal amounts of H_2O_2 were present. The results shown in Figure 10 reveal that the signals recorded from all three systems present similar eight-line spectra with a signal intensity ratio of 1:2:2:1:1:2:2:1. On the basis of the literature data,[35,36] this spectrum ($a^P = 47.5$ G, $a^N = 14.1$ G, $a^H = 13.7$ G) was assigned to the DEPMPO−hydroxyl adduct. Although the results shown in Figure 10 also suggest that the acetate buffer and the leaching solution from the phosphate buffer containing Fe_3O_4 nanoparticles present quite comparable effects in generating the hydroxyl radical, the results shown in Figure 8 have demonstrated that nearly no polymerization of aniline occurred at pH 2.5 in the phosphate buffer in contrast to the acetate buffer. Therefore, it can be confirmed that acetate buffer plays a catalyzing role in the polymerization of aniline as demonstrated by the theoretical prediction shown in Figure 9. The results shown in Figure 10 further demonstrate that the leaching solution from the acetate buffer containing
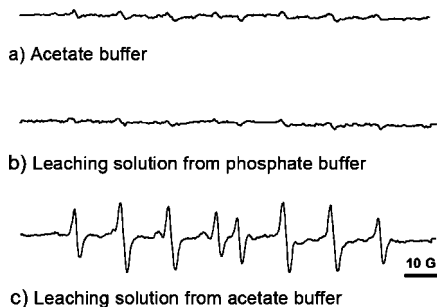
Figure 10. ESR signals recorded from acetate buffer (a), leaching solution from the phosphate buffer containing Fe$_3$O$_4$ nanoparticles (b), and leaching solution from the acetate buffer containing Fe$_3$O$_4$ nanoparticles (c). In all these three solutions equal amounts of H$_2$O$_2$ were presented.
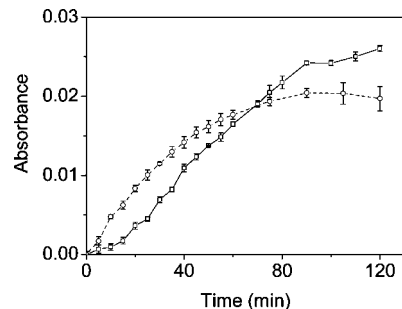

Figure 11. Temporal evolutions of the absorbance around 760 nm recorded from the polymerization of aniline taking place either in acetate buffer containing Fe$_3$O$_4$ nanoparticles (solid curve) or in their leaching solution (dashed curve).

Fe$_3$O$_4$ nanoparticles presents an enhanced signal much stronger than the sum of those from the former two solutions, suggesting that the carboxylic group and Fe ions take a synergistic effect in catalyzing the decomposition of H$_2$O$_2$ to generate hydroxyl radical.

Nature of the Peroxidase-like Activity of Fe$_3$O$_4$ Nanoparticles. The aforementioned results have clearly demonstrated that carboxylic acid such as acetic acid and succinic acid in the buffers can effectively catalyze the polymerization of aniline by forming stable complexes with both aniline and aniline radical cation. Moreover, it also offers help to Fe ions to accelerate the decomposition of H$_2$O$_2$ to generate hydroxyl radical.

The next important question that remains to be answered is whether the Fe$_3$O$_4$ particles take the catalyzing effect via Fe ions present in the reaction system due to the corrosion of Fe$_3$O$_4$ nanoparticles. In fact, the Fe ions are not sufficient to enable the polymerization reaction following the Fenton mechanism. For example, the concentration of Fe ions in phosphate was determined to be 12.9 μg/mL, while that in the acetate buffer was only of 3.7 μg/mL at pH 2.5. Nevertheless, with the help of carboxylic acid, Fe ions with the reduced concentration work more effectively than those in the phosphate buffer in generating hydroxyl radical as demonstrated by the ESR experiments.

To provide direct information on the role of Fe$_3$O$_4$ nanoparticles in the polymerization of aniline, a control reaction was carried out upon the use of the leaching solution from the acetate buffer containing Fe$_3$O$_4$ nanoparticles. The leaching solution was prepared by incubating 0.45 mg of Fe$_3$O$_4$ nanoparticles in 3 mL of acetate buffer (pH 2.5) for 10 min followed by ultrafiltration for 10 min to remove Fe$_3$O$_4$ nanoparticles. Detailed results shown in Figure 11 demonstrate that the leaching solution can not only catalyze the polymerization of aniline but also show quite comparable effects with that achieved in the presence of Fe$_3$O$_4$ nanoparticles, which strongly demonstrates that Fe$_3$O$_4$ nanoparticles catalyze the polymerization via Fe ions. Nevertheless, this phenomenon seems to be contradictory to the observation that peroxidase substrate TMB is not readily oxidized by H$_2$O$_2$ in the leaching solution as reported by ref 20. The main reason of this discrepancy can be attributed to the difference in the concentration of the leached Fe ions. Under the current experimental conditions, the concentration of the leached iron ions achieved at pH 2.5 was of 332 μg/L, much higher than that reported in ref 20. In the latter experiments, Fe$_3$O$_4$ particles were incubated in acetate buffer at pH 3.5, and the resultant concentration of Fe ions was of 21.2 $\pm$ 0.7 μg/L. As a matter of fact, the amount of leached iron ions from Fe$_3$O$_4$ particles is strongly pH-dependent.[33] Lower pH is obviously in favor of

higher concentration of leached Fe ions, while, as shown in Figure S2 of the Supporting Information, a higher concentration of Fe ion dramatically accelerates the polymerization of aniline, which further verifies that Fe ions take the catalytic effect rather than the mother Fe$_3$O$_4$ nanoparticles. In addition, the current experiments adopted much smaller Fe$_3$O$_4$ particles (11 nm) in contrast to 300 nm nanoparticles used in leaching ion experiments in ref 20, which should partly be responsible for the higher concentration of the leached Fe ions achieved in the current experiments. Because TMB and OPD, the typical chromogens for HRP, are simple derivatives of aniline, the above elucidated mechanism suggest that the peroxidase-like activity of Fe$_3$O$_4$ nanoparticles may not be true.

Conclusions

In summary, Fe$_3$O$_4$ nanoparticles were used to catalyze the polymerization of aniline, following previous reports on their "peroxidase-like" activity, to achieve PANI/Fe$_3$O$_4$ nanoparticle composite materials. The use of H$_2$O$_2$ as oxidant enabled the synthetic route to be facile and ecofriendly. Systematic experiments were performed to optimize the synthetic parameters. Preliminary results reveal that the resultant PANI/Fe$_3$O$_4$ nanoparticle composite possesses a thickness-dependent microwave absorption property. More detailed experiments by theoretical calculation in combination with ESR measurements reveal that carboxylic acid such as acetic acid and succinic acid can not only catalyze the polymerization of aniline by forming stable complexes with aniline and aniline radical cation but also catalyze the generation of hydroxyl radical via the decomposition of H$_2$O$_2$. Furthermore, carboxylic acid also presents synergistic effect with Fe ions in accelerating the generation of hydroxyl radical. As a matter of fact, the catalyzing effects of carboxylic acid in the polymerization of aniline or generation of hydroxyl radical were never reported before, even though different impacts of various types of organic acids on the polymerization of aniline were previously observed. However, the current investigations clearly elucidate the role of carboxylic acid in different stages of the polymerization of aniline, which should be very valuable for the chemical synthesis of polyaniline. Furthermore, the nature of the peroxidase-like activity was demonstrated to be synergistic catalyzing effects of both carboxylic acid and Fe ions. Nevertheless, PANI/Fe$_3$O$_4$ nanoparticle composite can still be prepared by taking the Fe$_3$O$_4$ nanoparticles as an "enzyme-mimic catalyst" even though previously proposed mechanism seems not relevant.

Supporting Information Available: Permittivity and permeability spectra of the as-prepared PANI/Fe$_3$O$_4$ nanoparticle composite, and temporal evolutions of the absorbance from the polymerization of aniline containing different concentrations of Fe ions. This material is available free of charge via the Internet at http://pubs.acs.org.

References and Notes

(1) Gomez-Romero, P. *Adv. Mater.* **2001**, *13*, 163.

(2) Anderson, M. R.; Mattes, B. R.; Reiss, H.; Kaner, R. B. *Science* **1991**, *252*, 1412.

(3) Kawaguchi, H. *Prog. Polym. Sci.* **2000**, *25*, 1171.

(4) Capadona, J. R.; Van Den Berg, O.; Capadona, L. A.; Schroeter, M.; Rowan, S. J.; Tyler, D. J.; Weder, C. *Nat. Nanotechnol.* **2007**, *2*, 765.

(5) Anand, J.; Palaniappan, S.; Sathyanarayana, D. N. *Prog. Polym. Sci.* **1998**, *23*, 993.

(6) MacDiarmid, A. G.; Chiang, J.-C.; Hapern, M.; Huang, W. S.; Mu, S. L.; Samasiri, N. L. C.; Wu, W. Q.; Yaniger, S. Z. *Mol. Cryst. Liq. Cryst.* **1985**, *121*, 173.

(7) Tigelaar, D. M.; Lee, W.; Bates, K. A.; Saprigin, A.; Prigodin, V. N.; Cao, X. L.; Nafie, L. A.; Platz, M. S.; Epstein, A. *J. Chem. Mater.* **2002**, *14*, 1430.

(8) Focke, W. W.; Wnek, G. E.; Wei, Y. *J. Phys. Chem.* **1987**, *91*, 5813.

(9) Pron, A.; Genoud, F.; Menardo, C.; Nechtschein, M. *Synth. Met.* **1988**, *24*, 193.

(10) Yasuda, A.; Shimidzu, T. *Polym. J.* **1993**, *25*, 329.

(11) Ding, H. J.; Liu, X. M.; Wan, M. X.; Fu, S. Y. *J. Phys. Chem. B* **2008**, *112*, 9289.

(12) Genies, E. M.; Tsintavis, C.; Syed, A. A. *Mol. Cryst. Liq. Cryst.* **1985**, *121*, 181.

(13) Zhu, H. P.; Mu, S. L. *Synth. Met.* **2001**, *123*, 293.

(14) Sun, Z. C.; Geng, Y. H.; Li, J.; Wang, X. H.; Jing, X. B.; Wang, F. S. *J. Appl. Polym. Sci.* **1999**, *72*, 1077.

(15) Xu, P.; Singh, A.; Kaplan, D. L. *Adv. Polym. Sci.* **2006**, *194*, 69.

(16) Liu, W.; Kumar, J.; Tripathy, S.; Senecal, K. J.; Samuelson, L. *J. Am. Chem. Soc.* **1999**, *121*, 71.

(17) Samuelson, L. A.; Anagnostopoulos, A.; Alva, K. S.; Kumar, J.; Tripathy, S. K. *Macromolecules* **1998**, *31*, 4376.

(18) Cholli, A. L.; Thiyagarajan, M.; Kumar, J.; Parmar, V. S. *Pure Appl. Chem.* **2005**, *77*, 339.

(19) Ryu, K. G.; Mceldoon, J. P.; Pokora, A. R.; Cyrus, W.; Dordick, J. S. *Biotechnol. Bioeng.* **1993**, *42*, 807.

(20) Gao, L. Z.; Zhuang, J.; Nie, L.; Zhang, J. B.; Zhang, Y.; Gu, N.; Wang, T. H.; Feng, J.; Yang, D. L.; Perrett, S.; Yan, X. *Nat. Nanotechnol.* **2007**, *2*, 577.

(21) Li, Z.; Wei, L.; Gao, M. Y.; Lei, H. *Adv. Mater.* **2005**, *17*, 1001.

(22) Barbati, S.; Clement, J. L.; Olive, G.; Roubaud, V.; Tuccio, B.; Tordo, P. In *Free Radicals in Biology and Environment*; Minisci, F., Ed.; Springer: London, 1997; p 39.

(23) Kang, E. T.; Neoh, K. G.; Tan, K. L. *Prog. Polym. Sci.* **1998**, *23*, 277.

(24) Liu, W.; Cholli, A. L.; Nagarajan, R.; Kumar, J.; Tripathy, S.; Bruno, F. F.; Samuelson, L. *J. Am. Chem. Soc.* **1999**, *121*, 11345.

(25) Liu, W.; Kumar, J.; Tripathy, S.; Samuelson, L. A. *Langmuir* **2002**, *18*, 9696.

(26) Stejskal, J.; Trchova, M.; Prokes, J.; Sapurina, I. *Chem. Mater.* **2001**, *13*, 4083.

(27) Jousseaume, V.; Morsli, M.; Bonnet, A.; Lefrant, S. *J. Appl. Polym. Sci.* **1998**, *67*, 1209.

(28) Qiu, G. H.; Wang, Q.; Nie, M. *J. Appl. Polym. Sci.* **2006**, *102*, 2107.

(29) Xu, P.; Han, X. J.; Jiang, J. J.; Wang, X. H.; Li, X. D.; Wen, A. H. *J. Phys. Chem. C* **2007**, *111*, 12603.

(30) Stejskal, J.; Hlavata, D.; Holler, P.; Trchova, M.; Prokes, J.; Sapurina, I. *Polym. Int.* **2004**, *53*, 294.

(31) Gok, A.; Sari, B. *J. Appl. Polym. Sci.* **2002**, *84*, 1993.

(32) Martyak, N. M. *Mater. Chem. Phys.* **2003**, *81*, 143.

(33) Wei, H.; Wang, E. *Anal. Chem.* **2008**, *80*, 2250.

(34) Wei, Y.; Hsueh, K. F.; Jang, G. W. *Polymer* **1994**, *35*, 3572.

(35) Singh, R. J.; Karoui, H.; Gunther, M. R.; Beckman, J. S.; Mason, R. P.; Kalyanaraman, B. *Proc. Natl. Acad. Sci. U.S.A.* **1998**, *95*, 6675.

(36) Karoui, H.; Hogg, N.; Frejaville, C.; Tordo, P.; Kalyanaraman, B. *J. Biol. Chem.* **1996**, *271*, 6000.

JP811125K